

This is an Open Access document downloaded from ORCA, Cardiff University's institutional repository:<https://orca.cardiff.ac.uk/id/eprint/118298/>

This is the author's version of a work that was submitted to / accepted for publication.

Citation for final published version:

Goswami, Subhadip, Nelson, Jordan N., Islamoglu, Timur, Wu, Yi-Lin , Farha, Omar K. and Wasielewski, Michael R. 2018. Photoexcited naphthalene diimide radical anion linking the nodes of a metal-organic framework: a heterogeneous super-reductant. *Chemistry of Materials* 30 (8) , pp. 2488-2492. 10.1021/acs.chemmater.8b00720

Publishers page: <http://dx.doi.org/10.1021/acs.chemmater.8b00720>

Please note:

Changes made as a result of publishing processes such as copy-editing, formatting and page numbers may not be reflected in this version. For the definitive version of this publication, please refer to the published source. You are advised to consult the publisher's version if you wish to cite this paper.

This version is being made available in accordance with publisher policies. See <http://orca.cf.ac.uk/policies.html> for usage policies. Copyright and moral rights for publications made available in ORCA are retained by the copyright holders.



Photoexcited Naphthalene Diimide Radical Anion Linking the Nodes of a Metal–Organic Framework: A Heterogeneous Super-reductant

Subhadip Goswami,^{†,#} Jordan N. Nelson,^{†,#} Timur Islamoglu,[†] Yi-Lin Wu,^{*,†,§,||} Omar K. Farha,^{*,†,‡,||} and Michael R. Wasielewski^{*,†,§,||}

[†]Department of Chemistry, Northwestern University, Evanston, Illinois 60208, United States

[§]Argonne–Northwestern Solar Energy Research (ANSER) Center, Northwestern University, Evanston, Illinois 60208, United States

^{||}Institute for Sustainability and Energy at Northwestern (ISEN), Northwestern University, Evanston, Illinois 60208, United States

[‡]Department of Chemistry, Faculty of Science, King Abdulaziz University, Jeddah 22254, Saudi Arabia

Aromatic organic anions are reactive species involved in various chemical transformations.^{1–4} The photochemistry and photophysics of these species have been the subject of

extensive study as they have been implicated in many photoinduced electron transfer processes, and are demonstrated to be powerful reducing agents.^{5–11} Such properties were substantiated by the observation of rapid electron ejection to give solvated electrons, electron–cation pairs, or reduced electron acceptors upon photolysis of aromatic anions (e.g., sodium pyrenide or biphenylide).^{5,7} Though most of the strongly photoreducing chromophores absorb in the UV or the blue part of the solar spectrum, aromatic anions tend to display absorption in the visible and near-infrared region, suggesting their potential for reductive artificial photosynthesis.

In particular, the naphthalene-1,8:4,5-bis(dicarboximide) radical anion (NDI^{•−}, E_{NDI(0)/NDI(1−)} ~ −0.5 V vs saturated calomel electrode, SCE) is electrochemically stable^{12,13} and absorbs from 400 to 800 nm, with absorption maxima at 470, 610, 700, and 780 nm.¹⁴ These properties suggest that the photoexcited state of NDI^{•−} should be a more powerful photoreductant with E_{NDI(0)/NDI(*,1−)} ~ −2.1 V, than the UV-absorbing [tris(2,2′-phenylpyridine)]iridium (fac-Ir(ppy)₃, E_{(+)/(*,0)} ~ −1.7 V),¹⁵ even reaching to the potential needed for energy-demanding direct CO₂ reduction (CO₂ + e[−] → [CO₂]^{•−}, E = −2.14 V).¹⁶ NDI^{•−} can be easily generated by electrochemical methods,¹⁴ mild reductants such as cobalto-cene (CoCp₂) or tetrakis(dimethylamino)ethylene (TDAE),^{17,18} or photoreduction of neutral NDI by alkyl-amines¹⁹ as the result of its low reduction potential. Efficient photoinduced electron transfer from the excited *NDI^{•−} to Re-based CO₂-reducing catalysts has been reported in covalent molecular dyads/triads, illustrating the potential of *NDI^{•−} as

18,20–22

an electron donor for solar fuels generation.

Recently, there has been growing interest in electrochemically active metal–organic frameworks (MOFs).²³ The high porosity of these materials imparts facile mass transport and ion conductivity, and the crystallinity ensures homogeneous chemical reactivity across the solids. Indeed, electrochromic behavior has been reported for NDI- and pyrene-based MOFs with fast color switching rates, and the donor–acceptor interactions between π-acidic NDI and electron rich molecules have been utilized to sense organic guests.^{24–33} The combination of powerful organic photoreductants and MOF

architecture is thus anticipated to provide an opportunity for reductive chemical transformations. Specifically, we report here the synthesis and characterization of an UiO-type MOF (UiO-NDI, Figure 1) composed of Zr₆-based metal node and linearly

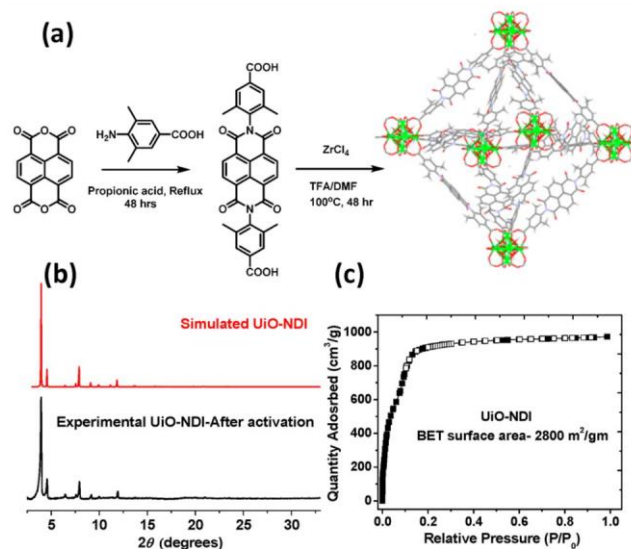


Figure 1. (a) Synthesis of UiO-NDI and the schematic representation of the octahedron cage in the MOF. Color code used for the Zr₆O₈ node cluster: Zr = green, O = red. (b) Comparison between the powder X-ray diffraction pattern of UiO-NDI, red = simulated, black = synthesized and after activation. (c) Nitrogen adsorption (■) and desorption (□) isotherms measured at 77 K, BET area is given.

disubstituted N,N-bis(2,6-dimethyl-4-benzoic acid)-NDI (NDI-COOH).³⁴ The Zr(IV) oxide-based structure was selected for its high chemical stability³⁵ and the meta-dimethyl groups in the NDI unit provide solubility for the MOF synthesis. The strong photoreducing power of the reduced MOF, UiO-NDI^{•−}, is tested against the reduction of chlorocarbon derivatives, a class of common pollutants resistant to reductive chemistry.

The formation of UiO-NDI MOF makes use of solvothermal synthesis in *N,N*-dimethylformamide (DMF) at 100 °C in the presence of trifluoroacetic acid as the modulator, NDI-COOH as the ligand, and ZrCl₄ as the metal source. The resultant octahedral crystals (~0.5 μm, Figure S2) exhibit powder X-ray diffraction patterns consistent with the predicted structures of the *fcu*-topology, the most common topology observed with ditopic linkers and Zr₆-based nodes (Figure 1b). The permanent porosity were supported by N₂ isotherm measurement at 77 K after supercritical CO₂ activation followed by heating at 120 °C under vacuum for 12 h; a type IV reversible isotherm with Brunauer–Emmett–Teller (BET) surface area of 2800 m² g⁻¹ was observed (Figure 1c).

The UV–vis spectrum of the suspension of UiO-NDI in DMF indicates the absorption <400 nm predominant from NDI (Figure 2a). It is important to note that the vibronic

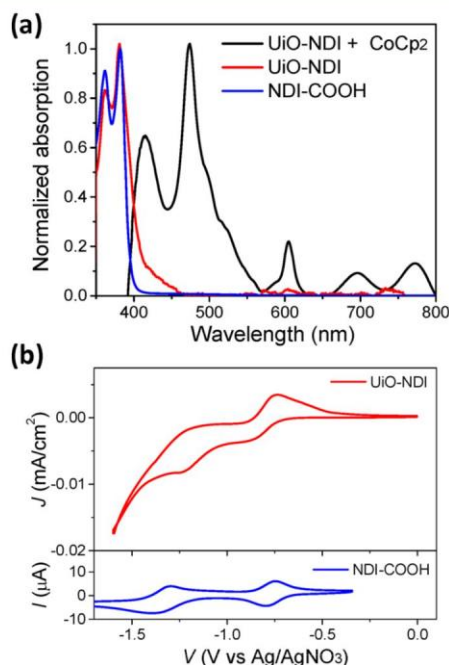


Figure 2. (a) UV–vis absorption spectra of the NDI ligand (blue line), UiO-NDI (red), and UiO-NDI^{•-} (black) generated by cobaltocene (CoCp₂). (b) Cyclic voltammograms of UiO-NDI measured in the solution of 1 M nBu₄NPF₆ in CH₂Cl₂ (red line) and the NDI linker (1 mM) in the solution of 0.1 M nBu₄NPF₆ in DMF (blue).

progression (0-0 band around 380 nm and 0-1 band around 360 nm) commonly observed for monomeric NDI derivatives is well resolved, indicative of minimal electronic coupling between neighboring NDIs. Such an observation is consistent with the long centroid-to-centroid distance of 13.6 Å between NDIs according to the structural model. Similarly, when the suspension of UiO-NDI was reduced by CoCp₂, monomer-like UV–vis absorption of NDI radical anions was observed. The electrochemical behavior of UiO-NDI was examined by cyclic voltammetry; the samples were prepared by electrophoretic deposition (EPD) on fluorine-doped tin oxide (FTO) substrates from suspended MOF samples in toluene. Once again, the typical monomer-like, two one-electron reduction waves of NDI were observed (Figure 2b). These observations are significant in that incorporation of redox active sites within MOF structures preserves the electronic properties of the individual chromophore, and the otherwise energy-dissipating

H-/J-aggregate or excimer formation is prohibited. The combination of UV–vis and electrochemical data suggest that the -2.1 V vs SCE photoreducing power is maintained in UiO-NDI^{•-}.

Figure 3 summarizes the results of electron paramagnetic resonance (EPR) spectroscopy used to probe the spin

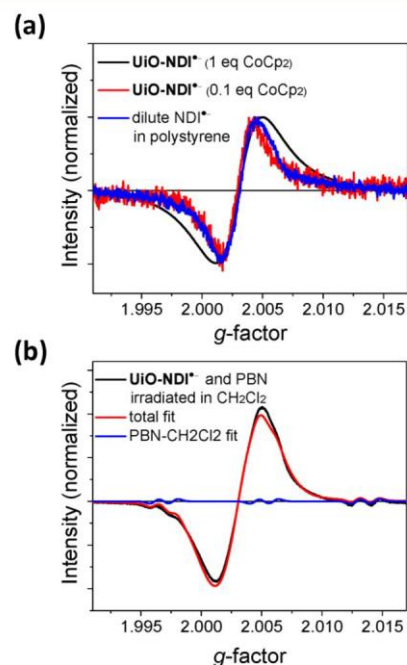


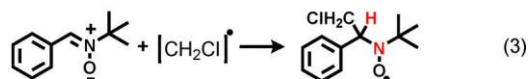
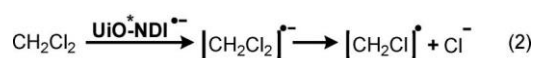
Figure 3. (a) CW-EPR spectra of NDI^{•-} diluted in a polystyrene matrix and UiO-NDI chemically reduced with 1 and 0.1 equiv CoCp₂. (b) CW-EPR spectra of reduced UiO-NDI (1 equiv CoCp₂) soaked in CH₂Cl₂ illuminated with 480 nm light (15 mW average power) for 2 h in the presence of *N*-tert-butyl- α -phenylnitrene (PBN) spin trap. The total fit (two components) of the spectrum is shown along with the minor component attributed to the PBN spin adduct.

distribution of the reduced UiO-NDI^{•-} MOF. The singly reduced NDI radical anion was generated with CoCp₂ in a minimal amount of CH₂Cl₂. The broad radical signal in the continuous-wave (CW) EPR spectrum is the result of NDI^{•-} in a randomly oriented solid state, as would be expected from the UiO-NDI crystalline powders. To test the possibility of electron-hopping between the NDI units in the MOF,^{36–38} varying equivalents of CoCp₂ were investigated, but the CW-EPR spectra of UiO-NDI^{•-} remain essentially unchanged. The slightly larger width for fully reduced UiO-NDI^{•-} is likely due to a general increase in spin density, resulting a reduction of transverse relaxation lifetime (T_2) and, inversely, an increase in line width.³⁹ A significant decrease in the spectral width of UiO-NDI^{•-} at lower concentrations of NDI^{•-} (fewer equivalents of CoCp₂) was not observed, concluding the radical is not delocalized between NDI units on the EPR time scale. Instead, the spectrum of UiO-NDI^{•-} in the latter case remains comparable to that of dilute NDI^{•-} in polystyrene. Additionally, no wide-field spectra were observed in any case, precluding the influence of Zr nuclei on NDI^{•-}. This result indicates that the electronic behavior of NDI^{•-} as a linker in the MOF is comparable to that of isolated NDI^{•-}. The excited NDI^{•-} in the MOF structure is therefore unlikely to be quenched by interactions between neutral and reduced NDI.

With the properties of the neutral and reduced forms of UiO-NDI characterized, its photochemical reactivity was tested by attempting to reduce CH₂Cl₂. Such a solvent was chosen as the target not only because of its conventional use in dissolving and delivering CoCp₂ for UiO-NDI^{•-} generation, but it also represents one of the most difficult pollutant substrates to be removed by reductive degradation.^{40,41} Whereas the reduction potential of chlorinated hydrocarbons often exhibits some degree of electrode-dependence,^{40,42, 43} the reduction on-set was measured to be -2.0 V vs SCE on a glassy carbon electrode (Figure S3),^{40,44} and most highly chlorinated aliphatic or aromatic hydrocarbons exhibit milder reduction potentials.

To monitor the photoreduction process, samples of UiO-NDI^{•-} were irradiated with 480 nm light in the presence of CH₂Cl₂ and N-tert-butyl- α -phenylnitron (PBN). The latter compound is known to react with short-lived and reactive radical species ("spin trapping") by forming a longer-lived spin adduct with the radical as described in Scheme 1. The

Scheme 1. Mechanism of CH₂Cl₂ Reduction by Photoexcited UiO-NDI^{•-} Radical Anions and N-tert-butyl- α -phenylnitron (PBN)-Spin Adduct Formation^a



^aHyperfine-contributing nuclei of primary interest are highlighted in red.

characteristic electron-nuclear hyperfine coupling constants of the nitroxide nitrogen and benzyl hydrogen in the radical spin adduct can be used to identify the radical that has been generated and trapped.⁴⁵ Upon irradiation at 200 K, a new set of EPR radical signal is observed on top of the central feature of UiO-NDI^{•-} (most noticeable at $g \sim 1.995$ and 2.015 , Figure 3b). This radical has the splitting pattern indicative of principally one N and one H hyperfine interaction, as is expected from a PBN spin adduct. The temperature of 200 K was selected to maximize the lifetime of the transient radical, but remain well above of the freezing point of CH₂Cl₂; the analogous experiment performed in frozen CH₂Cl₂ at 85 K did not yield spin-trap signals, implying a diffusion-limited reaction.

Though the central portion of the feature attributed to the spin adduct overlaps with that of UiO-NDI^{•-}, the distortion of the derivative shape of the main signal is clearly visible, and the fit to the feature attributed to the spin adduct alone is shown in Figure 3b. Previous cathodic electrochemical investigations of chlorinated aliphatic hydrocarbons have suggested that the reduction should result in the two-step or concerted liberation of mineralized Cl⁻ ions and a carbon-based free radical (Scheme 1, eq 2).^{40,41} The observed spin-trap product shows hyperfine constants ($a_N = 1.45$ mT and $a_H = 0.27$ mT) that are in a good agreement with that of the reported PBN spin adduct of the $\dot{\text{C}}\text{H}_2\text{Cl}$ radical ($a_N = 1.429$ mT and $a_H = 0.291$ mT) generated in CH₂Cl₂ by photolysis of an azido-Pd(II) complex.⁴⁶ In comparison, the formation of this radical adduct was not observed from 480 nm photoexcitation of PBN on its own in CH₂Cl₂ or of the sample containing both UiO-NDI^{•-}

and PBN in tetrahydrofuran (THF) in place of CH₂Cl₂. When UiO-NDI^{•-} was irradiated in CH₂Cl₂ in the absence of PBN, no spectral change was observed after exposure to light at 298, 200, or 85 K. When a solution of the reduced NDI ligand and PBN in CH₂Cl₂ were irradiated at 480 nm, the radical adduct was not observed, either (Figure S4).

The weak spin-adduct EPR signal compared to that of UiO-NDI^{•-} could be due in part to the transient nature of the $\dot{\text{C}}\text{H}_2\text{Cl}$ radical and, perhaps more importantly, to the short photoexcited state lifetime of $^*\text{NDI}^{\bullet-}$ (140 ps)¹⁴ that competes inefficiently with diffusional intermolecular electron-transfer reactions. The intermolecular electron-transfer rate may be enhanced by the use of a cationic redox mediator^{47,48} by virtue of favorable Coulombic interactions. Nevertheless, the detection of the $\dot{\text{C}}\text{H}_2\text{Cl}$ radical is strong evidence for the potential of the UiO-NDI^{•-} MOF for carrying out energy-demanding reduction processes. The absence of spin-adduct formation by the $^*[\text{NDI-COOH}]^{\bullet-}$ ligand in CH₂Cl₂, likely due to intermolecular deactivation, shows the advantage of UiO-NDI MOF as a super-reductant.

In summary, we have demonstrated that a crystalline and porous Zr(IV)-based UiO-NDI MOF scaffold can be utilized to incorporate strongly photoreducing chromophores. The wide spacing between chromophores and the weak electronic coupling through space or the Zr₆ nodes prevent deactivation of the excited state and thus preserve the monomer-like photochemical reactivity. The strong photoreducing power of UiO-NDI^{•-} was evidenced by the reductive degradation of CH₂Cl₂. This work also suggests that a promising catalytic photoreduction scheme can be envisaged by rapid electrochemical regeneration of UiO-NDI^{•-} on FTO.^{24,27}

ASSOCIATED CONTENT

* Supporting Information

Instrumental techniques, synthesis, PXRD and pore size distributions, SEM images, electrophoretic depositions of UiO-NDI films, electrochemistry of CH₂Cl₂, and additional EPR spectra (PDF)

AUTHOR INFORMATION

Corresponding Authors

*yi-lin.wu@northwestern.edu (Y.-L.W.).

*o-farha@northwestern.edu (O.K.F.).

*m-wasielewski@northwestern.edu (M.R.W.).

ORCID

Subhadip Goswami: 0000-0002-8462-9054

Timur Islamoglu: 0000-0003-3688-9158

Yi-Lin Wu: 0000-0003-0253-1625

Omar K. Farha: 0000-0002-9904-9845

Michael R. Wasielewski: 0000-0003-2920-5440

Author Contributions

#S.G. and J.N.N. contributed equally.

Funding

This work was supported by the Argonne Northwestern Solar Energy Research (ANSER) Center, an Energy Frontier Research Center funded by the U.S. Department of Energy (DOE), Office of Science, Office of Basic Energy Sciences, under award number DE-SC0001059 (NDI excited state

chemistry). O.K.F. gratefully acknowledges the support of the Nanoporous Materials Genome Center, funded by the U.S. DOE, Office of Science, Basic Energy Sciences Program (Award DE-FG02-17ER16362) (MOF design).

Notes

The authors declare no competing financial interest.

ACKNOWLEDGMENTS

We thank Diego Gomez-Gualdrón (Colorado School of Mines) for the simulation of the UiO-NDI structure.

REFERENCES

- (1) Holy, N. L. Reactions of Radical-Anions and Dianions of Aromatic-Hydrocarbons. *Chem. Rev.* 1974, 74, 243–277.
- (2) Jensen, B. S.; Parker, V. D. Reactions of Aromatic Anion Radicals and Dianions 0.2. Reversible Reduction of Anion Radicals to Dianions. *J. Am. Chem. Soc.* 1975, 97, 5211–5217.
- (3) Nguyen, J. D.; D'Amato, E. M.; Narayanam, J. M. R.; Stephenson, C. R. J. Engaging unactivated alkyl, alkenyl and aryl iodides in visible-light-mediated free radical reactions. *Nat. Chem.* 2012, 4, 854–859.
- (4) Meijere, A. d.; Bräse, S.; Oestreich, M. *Metal-catalyzed cross-coupling reactions and more*; Wiley-VCH: Weinheim, Germany, 2014.
- (5) Fox, M. A. Photoexcited States of Organic-Anions. *Chem. Rev.* 1979, 79, 253–273.
- (6) Shukla, S. S.; Rusling, J. F. Photoelectrocatalytic Reduction of 4-Chlorobiphenyl Using Anion Radicals and Visible-Light. *J. Phys. Chem.* 1985, 89, 3353–3358.
- (7) Soumillon, J. P. *Top. Curr. Chem.* 1993, 168, 93–141.
- (8) Eggins, B. R.; Robertson, P. K. J. Photoelectrochemistry Using Quinone Radical-Anions. *J. Chem. Soc., Faraday Trans.* 1994, 90, 2249–2256.
- (9) Robertson, P. K. J.; Eggins, B. R. Photoelectrochemistry with Quinone Radical-Anions Photoassisted Reduction of Halobenzenes and Carbonyl-Compounds. *J. Chem. Soc., Perkin Trans. 2* 1994, 1829–1832.
- (10) Leslie, W. M.; Compton, R. G.; Silk, T. Photoelectrochemical reaction mechanisms. The photoelectrocatalytic reduction of 4-chlorobiphenyl. *J. Phys. Chem.* 1996, 100, 20114–20121.
- (11) Horke, D. A.; Li, Q. S.; Blancafort, L.; Verlet, J. R. R. Ultrafast above-threshold dynamics of the radical anion of a prototypical quinone electron-acceptor. *Nat. Chem.* 2013, 5, 711–717.
- (12) Kumar, S.; Ajayakumar, M. R.; Hundal, G.; Mukhopadhyay, P. Extraordinary Stability of Naphthalenediimide Radical Ion and Its Ultra-Electron-Deficient Precursor: Strategic Role of the Phosphonium Group. *J. Am. Chem. Soc.* 2014, 136, 12004–12010.
- (13) Heywang, G.; Born, L.; Fitzky, H. G.; Hassel, T.; Hocker, J.; Müller, H. K.; Pittel, B.; Roth, S. Radical-Anion Salts of Naphthalenetetracarboxylic Acid-Derivatives - a Novel Class of Electrically Conducting Compounds. *Angew. Chem., Int. Ed. Engl.* 1989, 28, 483–485.
- (14) Gosztola, D.; Niemczyk, M. P.; Svec, W.; Lukas, A. S.; Wasielewski, M. R. Excited doublet states of electrochemically generated aromatic imide and diimide radical anions. *J. Phys. Chem. A* 2000, 104, 6545–6551.
- (15) Teegardin, K.; Day, J. I.; Chan, J.; Weaver, J. Advances in Photocatalysis: A Microreview of Visible Light Mediated Ruthenium and Iridium Catalyzed Organic Transformations. *Org. Process Res. Dev.* 2016, 20, 1156–1163.
- (16) Kumar, B.; Llorente, M.; Froehlich, J.; Dang, T.; Sathrum, A.; Kubiak, C. P. Photochemical and Photoelectrochemical Reduction of CO₂. *Annu. Rev. Phys. Chem.* 2012, 63, 541–569.
- (17) Wu, Y.; Krzyaniak, M. D.; Stoddart, J. F.; Wasielewski, M. R. Spin Frustration in the Triradical Trianion of a Naphthalenediimide Molecular Triangle. *J. Am. Chem. Soc.* 2017, 139, 2948–2951.
- (18) Fujitsuka, M.; Kim, S. S.; Lu, C.; Tojo, S.; Majima, T. Intermolecular and Intramolecular Electron Transfer Processes from Excited Naphthalene Diimide Radical Anions. *J. Phys. Chem. B* 2015, 119, 7275–7282.
- (19) Reiner, B. R.; Foxman, B. M.; Wade, C. R. Electrochemical and structural investigation of the interactions between naphthalene diimides and metal cations. *Dalton Trans.* 2017, 46, 9472–9480.
- (20) Lu, C.; Fujitsuka, M.; Sugimoto, A.; Majima, T. Dual Character of Excited Radical Anions in Aromatic Diimide Bis(radical anion)s: Donor or Acceptor? *J. Phys. Chem. C* 2017, 121, 4558–4563.
- (21) Martinez, J. F.; La Porte, N. T.; Mauck, C. M.; Wasielewski, M. R. Photo-driven electron transfer from the highly reducing excited state of naphthalene diimide radical anion to a CO₂ reduction catalyst within a molecular triad. *Faraday Discuss.* 2017, 198, 235–249.
- (22) La Porte, N. T.; Martinez, J. F.; Hedstrom, S.; Rudsteyn, B.; Phelan, B. T.; Mauck, C. M.; Young, R. M.; Batista, V. S.; Wasielewski, M. R. Photoinduced electron transfer from rylenediimide radical anions and dianions to Re(bpy)(CO)₃ using red and near-infrared light. *Chem. Sci.* 2017, 8, 3821–3831.
- (23) D'Alessandro, D. M. Exploiting redox activity in metal-organic frameworks: concepts, trends and perspectives. *Chem. Commun.* 2016, 52, 8957–8971.
- (24) Wade, C. R.; Li, M. Y.; Dinca, M. Facile Deposition of Multicolored Electrochromic Metal-Organic Framework Thin Films. *Angew. Chem., Int. Ed.* 2013, 52, 13377–13381.
- (25) Takashima, Y.; Martinez, V. M.; Furukawa, S.; Kondo, M.; Shimomura, S.; Uehara, H.; Nakahama, M.; Sugimoto, K.; Kitagawa, S. Molecular decoding using luminescence from an entangled porous framework. *Nat. Commun.* 2011, 2, Article number: 168. DOI: 10.1038/ncomms1170.
- (26) Kung, C. W.; Wang, T. C.; Mondloch, J. E.; Fairen-Jimenez, D.; Gardner, D. M.; Bury, W.; Klingsporn, J. M.; Barnes, J. C.; Van Duyne, R.; Stoddart, J. F.; Wasielewski, M. R.; Farha, O. K.; Hupp, J. T. Metal-Organic Framework Thin Films Composed of Free-Standing Acicular Nanorods Exhibiting Reversible Electrochromism. *Chem. Mater.* 2013, 25, 5012–5017.
- (27) AlKaabi, K.; Wade, C. R.; Dinca, M. Transparent-to-Dark Electrochromic Behavior in Naphthalene-Diimide-Based Mesoporous MOF-74 Analogs. *Chem.* 2016, 1, 264–272.
- (28) Mallick, A.; Garai, B.; Addicoat, M. A.; Petkov, P. S.; Heine, T.; Banerjee, R. Solid state organic amine detection in a photochromic porous metal organic framework. *Chem. Sci.* 2015, 6, 1420–1425.
- (29) Liu, J. J.; Shan, Y. B.; Fan, C. R.; Lin, M. J.; Huang, C. C.; Dai, W. X. Encapsulating Naphthalene in an Electron-Deficient MOF to Enhance Fluorescence for Organic Amines Sensing. *Inorg. Chem.* 2016, 55, 3680–3684.
- (30) Guo, Z.; Panda, D. K.; Gordillo, M. A.; Khatun, A.; Wu, H.; Zhou, W.; Saha, S. Lowering Band Gap of an Electroactive Metal-Organic Framework via Complementary Guest Intercalation. *ACS Appl. Mater. Interfaces* 2017, 9, 32413–32417.
- (31) Fang, X.; Yuan, X.; Song, Y. B.; Wang, J. D.; Lin, M. J. Cooperative lone pair- π and coordination interactions in naphthalene diimide coordination networks. *CrystEngComm* 2014, 16, 9090–9095.
- (32) Liu, J. J.; Hong, Y. J.; Guan, Y. F.; Lin, M. J.; Huang, C. C.; Dai, W. X. Lone pair- π interaction-induced generation of non-interpenetrated and photochromic cuboid 3-D naphthalene diimide coordination networks. *Dalton Trans.* 2015, 44, 653–658.
- (33) Han, L.; Qin, L.; Xu, L. P.; Zhou, Y.; Sun, J. L.; Zou, X. D. A novel photochromic calcium-based metal-organic framework derived from a naphthalene diimide chromophore. *Chem. Commun.* 2013, 49, 406–408.
- (34) Nelson, A. P.; Farha, O. K.; Mulfort, K. L.; Hupp, J. T. Supercritical Processing as a Route to High Internal Surface Areas and Permanent Microporosity in Metal-Organic Framework Materials. *J. Am. Chem. Soc.* 2009, 131, 458–460.
- (35) Bosch, M.; Zhang, M.; Zhou, H.-C. Increasing the Stability of Metal-Organic Frameworks. *Adv. Chem.* 2014, 2014, 8.
- (36) Wu, Y.; Nalluri, S. K. M.; Young, R. M.; Krzyaniak, M. D.; Margulies, E. A.; Stoddart, J. F.; Wasielewski, M. R. Charge and Spin Transport in an Organic Molecular Square. *Angew. Chem., Int. Ed.* 2015, 54, 11971–11977.

- (37) Wu, Y.; Frascioni, M.; Gardner, D. M.; McGonigal, P. R.; Schneebeli, S. T.; Wasielewski, M. R.; Stoddart, J. F. Electron Delocalization in a Rigid Cofacial Naphthalene-1,8:4,5-bis-(dicarboximide) Dimer. *Angew. Chem., Int. Ed.* 2014, **53**, 9476–9481.
- (38) Solomek, T.; Powers-Riggs, N. E.; Wu, Y.-L.; Young, R. M.; Krzyaniak, M. D.; Horwitz, N. E.; Wasielewski, M. R. Electron Hopping and Charge Separation within a Naphthalene-1,4:5,8-bis(dicarboximide) Chiral Covalent Organic Cage. *J. Am. Chem. Soc.* 2017, **139**, 3348–3351.
- (39) Weil, J. A.; Bolton, J. R. *Electron paramagnetic resonance: elementary theory and practical applications*, 2nd ed.; Wiley-Interscience: Hoboken, NJ, 2007.
- (40) Costentin, C.; Robert, M.; Saveant, J. M. Successive removal of chloride ions from organic polychloride pollutants. Mechanisms of reductive electrochemical elimination in aliphatic gem-polychlorides, alpha,beta-polychloroalkenes, and alpha,beta-polychloroalkanes in mildly protic medium. *J. Am. Chem. Soc.* 2003, **125**, 10729–10739.
- (41) Martin, E. T.; McGuire, C. M.; Mubarak, M. S.; Peters, D. G. Electroreductive Remediation of Halogenated Environmental Pollutants. *Chem. Rev.* 2016, **116**, 15198–15234.
- (42) Scialdone, O.; Guarisco, C.; Galia, A.; Herbois, R. Electroreduction of aliphatic chlorides at silver cathodes in water. *J. Electroanal. Chem.* 2010, **641**, 14–22.
- (43) Rondinini, S.; Vertova, A. Electrocatalysis on silver and silver alloys for dichloromethane and trichloromethane dehalogenation. *Electrochim. Acta* 2004, **49**, 4035–4046.
- (44) Fukui, K.; Morokuma, K.; Kato, H.; Yonezawa, T. The Polarographic Reduction and Electronic Structures of Organic Halides. *Bull. Chem. Soc. Jpn.* 1963, **36**, 217–222.
- (45) Janzen, E. G. Spin Trapping. *Acc. Chem. Res.* 1971, **4**, 31–40.
- (46) Hennig, H.; Stich, R.; Rehorek, D.; Thomas, P.; Kemp, T. J. Spin trapping of radicals formed during the photolysis of azidopalladium(II) and azidoplatinum(II) complexes. *Inorg. Chim. Acta* 1988, **143**, 7–8.
- (47) Van der Zee, F. R.; Cervantes, F. J. Impact and application of electron shuttles on the redox (bio)transformation of contaminants: A review. *Biotechnol. Adv.* 2009, **27**, 256–277.
- (48) Norris, M. R.; Concepcion, J. J.; Harrison, D. P.; Binstead, R. A.; Ashford, D. L.; Fang, Z.; Templeton, J. L.; Meyer, T. J. Redox Mediator Effect on Water Oxidation in a Ruthenium-Based Chromophore-Catalyst Assembly. *J. Am. Chem. Soc.* 2013, **135**, 2080–2083.